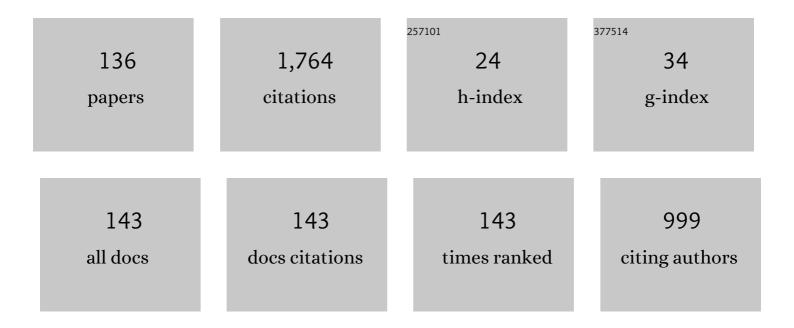
List of Publications by Year in descending order

Source: https://exaly.com/author-pdf/1902441/publications.pdf Version: 2024-02-01



#	Article	IF	CITATIONS
1	Universal self-field critical current for thin-film superconductors. Nature Communications, 2015, 6, 7820.	5.8	78
2	Enhanced flux pinning by BaZrO3 nanoparticles in metal-organic deposited YBCO second-generation HTS wire. Physica C: Superconductivity and Its Applications, 2008, 468, 183-189.	0.6	57
3	Compact high-voltage generator of primary power based on shock wave depolarization of lead zirconate titanate piezoelectric ceramics. Review of Scientific Instruments, 2004, 75, 2766-2769.	0.6	51
4	Flux pinning by discontinuous columnar defects in 74MeV Ag-irradiated YBa2Cu3O7 coated conductors. Physica C: Superconductivity and Its Applications, 2009, 469, 2060-2067.	0.6	46
5	Hole doping dependence of critical current density in YBa2Cu3O7â^îr´ conductors. Applied Physics Letters, 2014, 104, .	1.5	45
6	Longitudinal-shock-wave compression of Nd2Fe14B high-energy hard ferromagnet: The pressure-induced magnetic phase transition. Applied Physics Letters, 2003, 82, 1248-1250.	1.5	44
7	On the origin of critical temperature enhancement in atomically thin superconductors. 2D Materials, 2017, 4, 025072.	2.0	44
8	Transverse shock wave demagnetization of Nd2Fe14B high-energy hard ferromagnetics. Journal of Applied Physics, 2002, 92, 159-162.	1.1	43
9	Depolarization mechanisms of PbZr0.52Ti0.48O3 and PbZr0.95Ti0.05O3 poled ferroelectrics under high strain rate loading. Applied Physics Letters, 2014, 104, .	1.5	43
10	TEM observation of the microstructure of metal-organic deposited YBa ₂ Cu ₃ O _{7â^î} with Dy additions. Superconductor Science and Technology, 2007, 20, 880-885.	1.8	38
11	Thermodynamic Parameters of Single―or Multiâ€Band Superconductors Derived from Selfâ€Field Critical Currents. Annalen Der Physik, 2017, 529, 1700197.	0.9	37
12	Ultracompact explosive-driven high-current source of primary power based on shock wave demagnetization of Nd2Fe14B hard ferromagnetics. Review of Scientific Instruments, 2002, 73, 2738-2742.	0.6	36
13	Critical current anisotropy for second generation HTS wires. Current Applied Physics, 2008, 8, 388-390.	1.1	35
14	London penetration depth and thermal fluctuations in the sulphur hydride 203 K superconductor. Annalen Der Physik, 2017, 529, 1600390.	0.9	33
15	Ultrahigh energy density harvested from domain-engineered relaxor ferroelectric single crystals under high strain rate loading. Scientific Reports, 2017, 7, 46758.	1.6	32
16	Currents produced by explosive driven transverse shock wave ferromagnetic source of primary power in a coaxial single-turn seeding coil of a magnetocumulative generator. Journal of Applied Physics, 2003, 93, 4529-4535.	1.1	31
17	The development of a Roebel cable based 1 MVA HTS transformer. Superconductor Science and Technology, 2012, 25, 014002.	1.8	31
18	Classifying superconductivity in Moiré graphene superlattices. Scientific Reports, 2020, 10, 212.	1.6	28

EVGENY F TALANTSEV

#	Article	IF	CITATIONS
19	Classifying superconductivity in compressed H3S. Modern Physics Letters B, 2019, 33, 1950195.	1.0	27
20	Compact explosive-driven generator of primary power based on a longitudinal shock wave demagnetization of hard ferri- and ferromagnets. IEEE Transactions on Plasma Science, 2002, 30, 1681-1691.	0.6	26
21	Theoretical treatment of explosive-driven ferroelectric generators. IEEE Transactions on Plasma Science, 2002, 30, 1665-1673.	0.6	25
22	Completely explosive ultracompact high-voltage nanosecond pulse-generating system. Review of Scientific Instruments, 2006, 77, 043904.	0.6	25
23	Universal scaling of the self-field critical current in superconductors: from sub-nanometre to millimetre size. Scientific Reports, 2017, 7, 10010.	1.6	25
24	Shock wave demagnetization of BaFe12O19 hard ferrimagnetics. Journal of Applied Physics, 2002, 91, 3007-3009.	1.1	24
25	A Novel On-Chip Diagnostic Method to Measure Burn Rates of Energetic Materials. Journal of Energetic Materials, 2006, 24, 1-15.	1.0	24
26	Electric breakdown of longitudinally shocked Pb(Zr0.52Ti0.48)O3 ceramics. Journal of Applied Physics, 2011, 110, .	1.1	24
27	Completely explosive pulsed power minisystem. Review of Scientific Instruments, 2003, 74, 225-230.	0.6	23
28	Modeling of Vortex Paths in HTS. IEEE Transactions on Applied Superconductivity, 2007, 17, 3684-3687.	1.1	23
29	Superconductivity emerging from a stripe charge order in IrTe2 nanoflakes. Nature Communications, 2021, 12, 3157.	5.8	23
30	Extension of thickness-dependent dielectric breakdown law on adiabatically compressed ferroelectric materials. Applied Physics Letters, 2013, 102, .	1.5	22
31	Nanoparticle additions for enhanced flux pinning in YBCO HTS films. Current Applied Physics, 2008, 8, 372-375.	1.1	21
32	Classifying hydrogen-rich superconductors. Materials Research Express, 2019, 6, 106002.	0.8	21
33	High Voltage Charging of a Capacitor Bank. IEEE Transactions on Plasma Science, 2008, 36, 44-51.	0.6	19
34	The scaling of transport AC losses in Roebel cables with varying strand parameters. Superconductor Science and Technology, 2014, 27, 075007.	1.8	19
35	Advanced McMillan's equation and its application for the analysis of highly-compressed superconductors. Superconductor Science and Technology, 2020, 33, 094009.	1.8	19
36	PZT 52/48 Depolarization: Quasi-Static Thermal Heating Versus Longitudinal Explosive Shock. IEEE Transactions on Plasma Science, 2010, 38, 1856-1863.	0.6	18

#	Article	IF	CITATIONS
37	Note: Miniature 120-kV autonomous generator based on transverse shock-wave depolarization of Pb(Zr0.52Ti0.48)O3 ferroelectrics. Review of Scientific Instruments, 2011, 82, 086107.	0.6	18
38	Mode I Delamination Testing of REBCO Coated Conductors via Climbing Drum Peel Test. IEEE Transactions on Applied Superconductivity, 2018, 28, 1-5.	1.1	18
39	Compact autonomous explosive-driven pulsed power system based on a capacitive energy storage charged by a high-voltage shock-wave ferromagnetic generator. Review of Scientific Instruments, 2006, 77, 066107.	0.6	17
40	Effective Low-Temperature Flux Pinning by Au Ion Irradiation in HTS Coated Conductors. IEEE Transactions on Applied Superconductivity, 2015, 25, 1-5.	1.1	17
41	Completely Explosive Autonomous High-Voltage Pulsed-Power System Based on Shockwave Ferromagnetic Primary Power Source and Spiral Vector Inversion Generator. IEEE Transactions on Plasma Science, 2006, 34, 1866-1872.	0.6	16
42	Miniature 100-kV Explosive-Driven Prime Power Sources Based on Transverse Shock-Wave Depolarization of PZT 95/5 Ferroelectric Ceramics. IEEE Transactions on Plasma Science, 2012, 40, 2512-2516.	0.6	16
43	Critical current retention of potted and unpotted REBCO Roebel cables under transverse pressure and thermal cycling. Superconductor Science and Technology, 2017, 30, 045014.	1.8	16
44	Transverse Explosive Shock-Wave Compression of Nd2Fe14B High-Energy Hard Ferromagnets: Induced Magnetic Phase Transition. AlP Conference Proceedings, 2006, , .	0.3	15
45	Oxygen Deficiency, Stacking Faults and Calcium Substitution in MOD YBCO Coated Conductors. IEEE Transactions on Applied Superconductivity, 2013, 23, 7200205-7200205.	1.1	15
46	p-wave superconductivity in iron-based superconductors. Scientific Reports, 2019, 9, 14245.	1.6	15
47	Note: Autonomous pulsed power generator based on transverse shock wave depolarization of ferroelectric ceramics. Review of Scientific Instruments, 2010, 81, 126102.	0.6	14
48	Critical de Broglie wavelength in superconductors. Modern Physics Letters B, 2018, 32, 1850114.	1.0	14
49	THE CONDUCTIVITY OF A LONGITUDINAL-SHOCK-WAVE-COMPRESSED Nd2Fe14B HARD FERROMAGNETICS. Modern Physics Letters B, 2002, 16, 545-554.	1.0	13
50	Classifying superconductivity in an infinite-layer nickelate Nd0.8Sr0.2NiO2. Results in Physics, 2020, 17, 103118.	2.0	13
51	The electron–phonon coupling constant and the Debye temperature in polyhydrides of thorium, hexadeuteride of yttrium, and metallic hydrogen phase III. Journal of Applied Physics, 2021, 130, .	1.1	13
52	Note: Utilizing Pb(Zr0.95Ti0.05)O3 ferroelectric ceramics to scale down autonomous explosive-driven shock-wave ferroelectric generators. Review of Scientific Instruments, 2012, 83, 076104.	0.6	12
53	The onset of dissipation in high-temperature superconductors: Self-field experiments. AIP Advances, 2017, 7, .	0.6	12
54	The electron-phonon coupling constant, Fermi temperature and unconventional superconductivity in the carbonaceous sulfur hydride 190 K superconductor. Superconductor Science and Technology, 2021, 34, 034001.	1.8	12

EVGENY F TALANTSEV

#	Article	IF	CITATIONS
55	The tensile strength of perfect LuBa2Cu3O7-xsingle crystals of submicrometre cross-sectional dimensions. Superconductor Science and Technology, 1994, 7, 491-494.	1.8	11
56	ATOMIC STRUCTURE OF SUPERCONDUCTOR YBa2Cu3O7-x IN FIELD ION MICROSCOPE. Journal De Physique Colloque, 1988, 49, C6-477-C6-481.	0.2	11
57	An approach to identifying unconventional superconductivity in highly-compressed superconductors. Superconductor Science and Technology, 2020, 33, 124001.	1.8	11
58	Miniature Explosively Driven High-Current Transverse-Shock-Wave Ferromagnetic Generators. IEEE Transactions on Plasma Science, 2010, 38, 1784-1793.	0.6	10
59	The depolarization of Pb(Zr0.52Ti0.48)O3 ferroelectrics by cylindrical radially expanding shock waves and its utilization for miniature pulsed power. Review of Scientific Instruments, 2011, 82, 054701.	0.6	10
60	Current distribution across type II superconducting films: a new vortex-free critical state. Scientific Reports, 2018, 8, 1716.	1.6	10
61	Resistive transition of hydrogen-rich superconductors. Superconductor Science and Technology, 2021, 34, 064001.	1.8	10
62	Anisotropy of flux pinning properties in superconducting (Li,Fe)OHFeSe thin films. Superconductor Science and Technology, 2020, 33, 114009.	1.8	10
63	Longitudinal Shock Wave Depolarization of Pb(Zr52Ti48)O3 Polycrystalline Ferroelectrics and their Utilization in Explosive Pulsed Power. AIP Conference Proceedings, 2006, , .	0.3	9
64	Electric discharge caused by expanding armatures in flux compression generators. Applied Physics Letters, 2009, 94, .	1.5	9
65	Relating Critical Currents to Defect Populations in Superconductors. IEEE Transactions on Applied Superconductivity, 2013, 23, 8001705-8001705.	1.1	9
66	Classifying superconductivity in ThH-ThD superhydrides/superdeuterides. Materials Research Express, 2020, 7, 016003.	0.8	9
67	The current mode of pulsed power generation in a moving magnet system. IEEE Transactions on Plasma Science, 2002, 30, 1674-1680.	0.6	8
68	Flux Pinning by Barium Stannate Nanoparticles in MOD YBCO Coated Conductors. IEEE Transactions on Applied Superconductivity, 2009, 19, 3140-3143.	1.1	8
69	The onset of dissipation in high-temperature superconductors: magnetic hysteresis and field dependence. Scientific Reports, 2018, 8, 14463.	1.6	8
70	Quantifying the Charge Carrier Interaction in Metallic Twisted Bilayer Graphene Superlattices. Nanomaterials, 2021, 11, 1306.	1.9	8
71	Completely Explosive Ultracompact High-Voltage Pulse Generating System. , 2005, , .		7
72	Compressed H3S, Superfluid Density and the Quest for Room-Temperature Superconductivity. Journal of Superconductivity and Novel Magnetism, 2018, 31, 619-624.	0.8	7

#	Article	IF	CITATIONS
73	Polar projections for big data analysis in applied superconductivity. AIP Advances, 2018, 8, .	0.6	7
74	Classifying Induced Superconductivity in Atomically Thin Dirac-Cone Materials. Condensed Matter, 2019, 4, 83.	0.8	7
75	Comparison of highly-compressed C2/m-SnH12 superhydride with conventional superconductors. Journal of Physics Condensed Matter, 2021, 33, 285601.	0.7	7
76	The dominance of non-electron–phonon charge carrier interaction in highly-compressed superhydrides. Superconductor Science and Technology, 2021, 34, 115001.	1.8	7
77	A disorder-sensitive emergent vortex phase identified in high-T _c superconductor (Li,Fe)OHFeSe. Superconductor Science and Technology, 2022, 35, 064007.	1.8	7
78	Single-shot, repetitive, and lifetime high-voltage testing of capacitors. IEEE Transactions on Plasma Science, 2002, 30, 1943-1949.	0.6	6
79	Depolarization of a Pb(Zr52Ti48)O3 Polycrystalline Piezoelectric Energy-Carrying Element of Compact Pulsed Power Generator by a Longitudinal Shock Wave. , 2005, , .		6
80	Weak-links criterion for pnictide and cuprate superconductors. Superconductor Science and Technology, 2018, 31, 124001.	1.8	6
81	Normal state interlayer conductivity in epitaxial Nd2–x Ce x CuO4 films deposited on SrTiO3 (110) single crystal substrates. Materials Research Express, 2019, 6, 096005.	0.8	6
82	Unconventional superconductivity in highly-compressed unannealed sulphur hydride. Results in Physics, 2020, 16, 102993.	2.0	6
83	Pulsed Charging of Capacitor Bank by Compact Explosive-Driven High-Voltage Primary Power Source Based on Longitudinal Shock Wave Depolarization of Ferroelectric Ceramics. , 2005, , .		5
84	Microstructure of metal-organic deposited YBa2Cu3O7â~ʾĨ´ wires with Dy and Zr additions observed by TEM. Current Applied Physics, 2008, 8, 262-265.	1.1	5
85	Low-Temperature Pinning Behavior of MOD YBCO Coated Conductors. IEEE Transactions on Applied Superconductivity, 2011, 21, 3214-3217.	1.1	5
86	High Voltage Generation With Transversely Shock-Compressed Ferroelectrics: Breakdown Field on Thickness Dependence. IEEE Transactions on Plasma Science, 2016, 44, 1919-1927.	0.6	5
87	Two-band induced superconductivity in single-layer graphene and topological insulator bismuth selenide. Superconductor Science and Technology, 2018, 31, 015011.	1.8	5
88	Evaluation of a practical level of critical current densities in pnictides and recently discovered superconductors. Superconductor Science and Technology, 2019, 32, 084007.	1.8	5
89	Electron–phonon coupling constant and BCS ratios in LaH _{10â^'y} doped with magnetic rare-earth element. Superconductor Science and Technology, 2022, 35, 095008.	1.8	5
90	Field ion microscopy investigation of the disorder-to-order transformation in FePd2Au after bombardment by Ar+ions. Philosophical Magazine A: Physics of Condensed Matter, Structure, Defects and Mechanical Properties, 1994, 70, 439-445.	0.8	4

#	Article	IF	CITATIONS
91	Ferrihydrite gels derived in the Fe(NO3)3·9H2O–C2H5OH–CH3CHCH2O ternary system. Journal of Non-Crystalline Solids, 2005, 351, 1426-1432.	1.5	4
92	Fluxâ€Pinning Centers In Metalâ€Organic Deposited YBCO Coated Conductors. AlP Conference Proceedings, 2009, , .	0.3	4
93	Electric field-free gas breakdown in explosively driven generators. Physics of Plasmas, 2010, 17, 074504.	0.7	4
94	Effect of shock front geometry on shock depolarization of Pb(Zr0.52Ti0.48)O3 ferroelectric ceramics. Review of Scientific Instruments, 2012, 83, 074702.	0.6	4
95	The Dependence of Transport AC Loss on Temperature and DC Parallel Magnetic Field in an Eight-Strand YBCO Roebel Cable. IEEE Transactions on Applied Superconductivity, 2013, 23, 5402604-5402604.	1.1	4
96	Cryogen-free 1kA-class <i>I_c</i> measurement system featuring an 8 T HTS magnet. Journal of Physics: Conference Series, 2014, 507, 022037.	0.3	4
97	Micromachining of a high-temperature superconductor for field ion microscopy. Journal of Micromechanics and Microengineering, 1993, 3, 87-89.	1.5	3
98	DC Self-Field Critical Current in Superconductor/Dirac-Cone Material/Superconductor Junctions. Nanomaterials, 2019, 9, 1554.	1.9	3
99	Classifying Charge Carrier Interaction in Highly Compressed Elements and Silane. Materials, 2021, 14, 4322.	1.3	3
100	FIELD ION MICROSCOPE STUDY OF HIGH-TEMPERATURE SUPERCONDUCTOR Nd1.85Ce0.15CuO4. Modern Physics Letters B, 1992, 06, 1029-1035.	1.0	2
101	Pulse Charging of Capacitor Bank by Explosive-Driven Shock Wave Ferroelectric Generator. , 2006, , .		2
102	Operation of the longitudinal shock wave ferroelectric generator charging a capacitor bank: Experiments and digital model. , 2007, , .		2
103	Nucleation And Growth Of Baâ \in Reduced Metal Organic Deposited YBCO Films. , 2009, , .		2
104	Dominant role of the explosively expanding armature on the initiation of electric discharge in magnetic flux compression generators. , 2009, , .		2
105	Formation of Nanoparticles in Zr and Dy Doped YBCO MOD Superconducting Films. Materials Science Forum, 2011, 700, 15-18.	0.3	2
106	Gas Breakdown Initiation in Explosive-Driven Pulsed Power Systems: Phenomenon and Possible Mechanisms. IEEE Transactions on Plasma Science, 2012, 40, 2501-2511.	0.6	2
107	The onset of dissipation in high-temperature superconductors: flux trap, hysteresis and in-field performance of multifilamentary Bi2Sr2Ca2Cu3O10+x wires. Materials Research Express, 2019, 6, 026002.	0.8	2
108	Angular dependence of the upper critical field in randomly restacked 2D superconducting nanosheets. Superconductor Science and Technology, 2019, 32, 015013.	1.8	2

#	ARTICLE	IF	CITATIONS
109	Double-valued strong-coupling corrections to Bardeen–Cooper–Schrieffer ratios. Superconductor Science and Technology, 2020, 33, 124003.	1.8	2
110	Method to extracting the penetration field in superconductors from DC magnetization data. Review of Scientific Instruments, 2022, 93, .	0.6	2
111	Field ion microscopy of high-temperature superconductors. Superconductor Science and Technology, 1995, 8, 593-604.	1.8	1
112	Operation of High-Voltage Transverse Shock Wave Ferromagnetic Generator in the Open Circuit and Charging Modes. , 2005, , .		1
113	Transformer-Type Seeding System of a Helical FCG Based on a Transverse Shock Wave Ferromagnetic Generator. , 2006, , .		1
114	A New Concept of Explosive Pulsed Power: Design of Macro Primary Power Sources Based on Elementary Miniature Shock-Wave Ferromagnetic Cells. , 2006, , .		1
115	Operation of the Longitudinal Shock Wave Ferroelectric Generator Charging a Capacitor Bank. , 2007, , .		1
116	Miniature 100-kV explosively driven prime power sources based on transverse shock-wave depolarization of Pb(Zr <inf>0.95</inf> Ti <inf>0.05</inf>)O <inf>3</inf> ferroelectric ceramics. , 2011, , .		1
117	Imaging of Electric-Field-Free Gas Breakdown. IEEE Transactions on Plasma Science, 2011, 39, 2386-2387.	0.6	1
118	Pinning Force Anisotropy for HTS Wires. Materials Science Forum, 2011, 700, 7-10.	0.3	1
119	High voltage generation with transversely shock compressed ferroelectrics: Thickness dependent law for breakdown field. , 2015, , .		1
120	Formation of an Ordered Structure in the 40Au–25.4Pd–34.6Cu Alloy (wt %). Physics of Metals and Metallography, 2018, 119, 1222-1228.	0.3	1
121	Thermodynamic parameters of atomically thin superconductors derived from the upper critical field. Superconductor Science and Technology, 0, , .	1.8	1
122	Atomic structure and phase state of quenched FePd 2 Au alloy after bombardment by Ar+ions. , 1994, , .		0
123	New Concept for Constructing an Autonomous Completely Explosive Pulsed Power System: Transverse Shock Wave Ferromagnetic Primary Power Source and Loop Flux Compression Amplifier. , 2006, , .		0
124	Compact Autonomous Completely Explosive Pulsed Power System Based on Transverse Shock Wave Demagnetization Of Nd <inf>2</inf> Fe <inf>14</inf> B and Magnetic Flux Compression. , 2006, , .		0
125	Explosive-Driven Mini-System Based on Shock Wave Ferromagnetic Seed Source and Loop Magnetic Flux Compression Generator. , 2007, , .		0
126	Analytical Method for Calculation of Currents Produced by Shock Wave Ferromagnetic Generators. , 2007, , .		0

#	Article	IF	CITATIONS
127	Compact Autonomous Completely Explosive Pulsed Power Systems. , 2007, , .		0
128	Compact autonomous completely explosive pulsed power system. , 2007, , .		0
129	Explosive-driven mini-system based on shock wave ferromagnetic seed source and loop magnetic flux compression generator. , 2007, , .		0
130	Analytical model for explosive-driven ultracompact shock-wave ferromagnetic generators. , 2007, , .		0
131	Operation of longitudinal shock wave ferroelectric generators in the resistance mode. , 2009, , .		0
132	Conductivity of explosively shocked potassium chloride. , 2009, , .		0
133	PZT 52/48 ferroelectric ceramics: Depolarization and electric breakdown under longitudinal explosive shock. , 2011, , .		0
134	Possible mechanisms for electric-field-free gas breakdown. , 2011, , .		0
135	Cooper pair trajectories in superconducting slab at self-field conditions. Modern Physics Letters B, 2021, 35, 2150226.	1.0	0
136	Piecewise Model with Two Overlapped Stages for Structure Formation and Hardening upon High-Pressure Torsion. Metallurgical and Materials Transactions A: Physical Metallurgy and Materials Science, 2021, 52, 4510-4517.	1.1	0